Conformations of Bridging Polyelectrolytes in Poor Solvent: Single-Chain Self-Consistent Field Calculations

Galen T. Pickett*,† and Anna C. Balazs‡

Department of Physics and Astronomy, California State University, Long Beach, 1250 Bellflower Boulevard, Long Beach, California 90840-3901, and Department of Chemical and Petroleum Engineering, University of Pittsburgh, 1249 Benedum Hall, Pittsburgh, Pennsylvania 15261

Received July 21, 2000. In Final Form: May 9, 2001

We report on numerical self-consistent field (SCF) calculations on the single-chain conformation of an electrostatically charged, yet poorly soluble, flexible polymer. We find numerical evidence that a "necklace of beads" conformation is self-organized and speculate that the predicted cascade of conformational transitions can be probed via a single-chain mechanical experiment with an atomic force microscope.

Introduction

With the advent of new experimental techniques involving atomic force microscopy (AFM) able to probe the mechanical response of individual polymers to imposed tension, a systematic study of the complicated, three-dimensional structure of interesting polymers is possible. Such experiments[1] give detailed mechanical information on the global statistical conformation of flexible macromolecules as well as a direct measurement of their important structural length scales. For example, applied tension[2] causes a reorganization of DNA[3] and polysaccharides.[4] The loads under which these reorganizations occur can be used as a tension benchmark and has proven useful in mechanical studies of the strength of individual covalent bonds.[5] Also, by pulling a single structural protein from its host membrane, the resulting force vs extension profile reflects the freeing and then the unraveling of the chain's secondary structures.[6] These methods have also been applied to the single-chain pullout of single homopolymers from a homopolymer matrix into a poor solvent,[7] one of the important mechanisms in the physical fracture of reinforced polymer blends.[8,9] Thus, these single-chain mechanical methods are capable of determining the native conformations of macromolecules by determining their response to an applied traction. A distinct advantage of these experiments is that they determine the detailed mechanical response of individual chains at a level of detail ideally suited to comparison with the theoretical tools of computational materials science.

There are obviously many choices available when designing such an experiment: the chain can be either biologically active or not, it can have specialized mesogenic side groups or a simple architecture, and the chain can either have an electric charge or not. In this paper, we focus on charged, flexible chains, as they are predicted[10,11] to undergo a striking structural rearrangement of their monomers as solvent quality is decreased. In good solvents, charged chains adsorb on an oppositely charged surface readily. By pulling these chains from their adsorbed layers,[12] the features of the electrolyte layer and the polyelectrolyte chain conformation become clear. In a poor solvent, however, the situation is markedly different because of a self-assembly of the chain into a "beaded-necklace" conformation (Figure 1). We focus in this paper on a numerical investigation of the conformations of poorly soluble, electrostatically charged, flexible homopolymers in a theoretical formalism closely mimicking single-chain experiments. Thus, this paper can be seen as a proof of

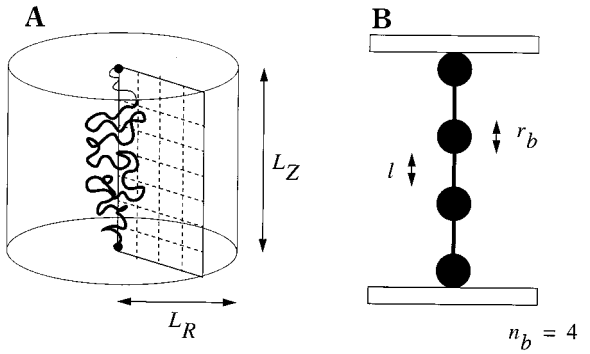

Figure 1. Schematic. In panel A, the schematic of the SCF calculations is presented. The polymer has N monomers, is flexible, and is uniformly charged with a charge/monomer given by αe, where e is the electron charge. One end of the chain is grafted at the center of the bottom circular plate, and the other is grafted at the center of the upper plate. A rectangular lattice is used to keep track of the cylindrical coordinates (r, z) labeling azimuthally equivalent points in space. The plates are held a distance L_Z apart, and the radii of both plates is L_R. In panel B, quantities of importance in the qualitative scaling theory are displayed: n_b is the number of beads on the conformation, each bead has a radius r_b, and each stretched string has a length l.

† California State University, Long Beach.

‡ University of Pittsburgh.

(1) Ortiz, C.; Hadziioannou, G. *Macromolecules* **1999**, *32*, 780.
(2) Reif, M.; Fernandez, J. M.; Gaub, H. E. *Phys. Rev. Lett.* **1998**, *81*, 4764.
(3) Smith, S. B.; Cui, Y.; Bustamante, C. *Science* **1996**, *271*, 795.
(4) Rief, M.; Oesterhelt, F.; Heymann, B.; Gaub, H. E. *Science* **1997**, *275*, 1295.
(5) Grandbois, M.; Beyer, M.; Reif, M.; Clausen-Schaumann, H.; Gaub, H. E. *Science* **1999**, *283*, 1727.
(6) Oesterhelt, F.; Oesterhelt, D.; Pfeiffer, M.; Engle, A.; Gaub, H. E.; Miller, D. J. *Science* **2000**, *288*, 143.
(7) Bemis, J. E.; Akhremitchev, B. B.; Walker, G. C. *Langmuir* **1999**, *15*, 2799.
(8) Pickett, G. T.; Jasnow, D.; Balazs, A. C. *Phys. Rev. Lett.* **1996**, *77*, 671.
(9) Sabouri-Ghomi, M.; Ispolatov, S.; Grant, M. *Phys. Rev. E: Stat. Phys., Plasmas, Fluids, Relat. Interdiscip. Top.* **1999**, *60*, 4460.
(10) Kantor, Y.; Kardar, M.; Ertas, D. *Physica A* (*Amsterdam*) **1997**, *249*, 301.
(11) Dobrynin, A. V.; Rubinstein, M.; Obukhov, S. P. *Macromolecules* **1996**, *28*, 2974. (b) Dobrynin, A. V.; Rubinstein, M. *Macromolecules* **1999**, *32*, 915.
(12) Châtellier, X.; Senden, T. J.; Joanny, J.-F.; di Meglio, J.-M. *Europhys. Lett.* **1998**, *41*, 303.

10.1021/la001034n CCC: $20.00
Published on Web 07/11/2001

principle that the well-established numerical self-consistent field (SCF) method of polymer physics can be successfully applied as a guide for experimentalists as they search for mechanical evidence detailing the self-organization of macromolecules. In particular, we investigate the complicated conformations of poorly soluble yet uniformly charged homopolymers and hope to reinforce the call[13,14] for an experimental investigation similar to that done on pullout[7] and adsorbed polyelectrolytes.[12]

These insoluble, charged polymers undergo an intriguing cascade of transitions whereby the chain conformation is characterized by charged globules connected by nearly fully stretched strands.[10,11] This scenario is amenable to further analytic treatment[15] and direct Monte Carlo investigation.[16,17] Our analysis will focus on the qualitative models of ref 11 as expanded in refs 13 and 14 and the numerical SCF calculations[18] on fully three-dimensional (yet highly symmetric) polyelectrolyte conformations. The stretching of "necklace" conformations has been recently subjected to a careful analysis in the context of scaling theories with realistic geometry-dependent prefactors faithfully accounted for,[13,14] and the main experimental signature of tension-induced necklace transitions is faithfully reproduced here (as in Figures 7 and 8): a characteristic sawtooth pattern in the tension vs separation response when the chain ends are held at a fixed distance and the chain tension is allowed to fluctuate. This situation can most commonly be arranged in a computer simulation or SCF calculation as we detail below. On the other hand, a plateau in the tension−separation profile should present itself in a process in which the tension is fixed and the distance between the chain ends is allowed to fluctuate. If the chain ends are connected to an immobile surface on one hand and the cantilever arm of an AFM on the other, the "constant-tension" scenario is to be expected under normal operating conditions for the AFM. That is, the tension in the cantilever is set, and the distance between the tip and the surface (and hence the distance between the chain ends) is measured. Thus, the experimental signature to be expected is a discontinuous jump in the plate separation at characteristic and repeatable tensions.

In our study, a single end-confined chain forms a bridge between the two substrates, and the structure adopted by the chain is qualitatively the same as free chains in bulk solution, as long as the separation between the plates is on the same scale as that of the elongated structures. The case of bridging chains is relevant to polymer-adsorption-induced gelation of a colloidal suspension, where the charged chains adsorb on the surfaces of the colloidal particles and naturally respond to any stress placed on the gel.

We first discuss the application of our numerical SCF lattice model to situations in which just a single polymer chain is being studied and then discuss the qualitative features of the cascade of necklace transitions that have been predicted.[11] Then, we demonstrate the cascade in our theoretical model and specify the direct, mechanical signature of the transition that can be looked for in a single-chain experiment. Finally, we make our conclusions and point to further work.

Model

The method of the SCF is a mature technique in polymer physics. The first numerical lattice models of this sort, by Scheutjens and Fleer,[19] rely on repeated applications of discrete recursion relations on a lattice to determine the profiles and statistics of adsorbing polymers. The current understanding of the diblock copolymer phase diagram[20] as well as the behavior of thin films of diblock and triblock copolymers[21,22] indicate that these and similar methods[23,24] are finding wide application.

All of these methods, however, rely upon the same division of labor in finding the equilibrium conformation of heavily entangled polymers: solving two coupled problems. First, given an external potential, U_A, that couples to the density of monomer species A, it is possible, numerically and on a lattice,[19] or off-lattice in a space of orthogonal functions of the required symmetry,[20] to determine the conformational statistics of a homopolymer composed of A monomers. That is, the statistical weight to be attributed to conformation can be determined.

What remains is to relate the potential U_A to the presence of all of the other chains in the system and to ensure that (usually, although by no means necessarily, especially when equation-of-state information[25] is available) an incompressibility constraint is matched

$$U_A(\vec{r}) = U_{hc}(\vec{r}) + \chi_{AB}\langle\phi_B\rangle + \text{other interactions} \quad (1)$$

with

$$\phi_A(\vec{r}) + \phi_B(\vec{r}) = 1 \quad (2)$$

Here, $U_{hc}(\vec{r})$ is a "hard-core" potential that affects all the monomers in the problem equally, and χ is the Flory−Huggins parameter describing the relative energy cost (in units of kT) to bring A and B monomers into contact. The function $\phi_B(\vec{r})$ is the spatial distribution of the fraction of the available space on lattice site $\vec{r}$ that is occupied by B monomers, and the angled brackets indicate a sum over nearest-neighbor lattice sites. Self-consistency is assured when $U_{hc}(\vec{r})$ can be determined, and U_A and U_B satisfy the self-consistency equation (eq 1). Also, each lattice site is completely filled with A and B monomers (eq 2). Once this is accomplished, it is possible to calculate all thermodynamic and structural information for the system.[19]

The application we have in mind here extends this concept. The usual justification for the self-consistency approximation is that a single chain encounters many more of its neighbors than itself and therefore exists in a mean field generated by the presence of its neighbors. Self-consistency is assured when the neighboring chains are forced to have the same statistics as the single chain under consideration. Our situation, shown schematically

(13) Tamashiro, M. N.; Schiessel, H. *Macromolecules* **2000**, *33*, 5263.
(14) Vilgis, T. A.; Johner, A.; Joanny, J. F. *Eur. Phys. J. E* **1999**, *2*, 289.
(15) Solis, F. J.; Olvera de la Cruz, M. *Macromolecules* **1998**, *31*, 5502.
(16) Micka, U.; Holm, C.; Kremer, K. *Langmuir* **1998**, *15*, 4033. (b) Micka, U.; Kremer, K. *Europhys. Lett.* **2000**, *49*, 189.
(17) Chodanowski, P.; Stoll, S. *J. Chem. Phys.* **1999**, *111*, 6069. (b) Lyulin, A. V.; Duenweg, B.; Borisov, O. V.; Darinskii, A. A. *Macromolecules* **1999**, *32*, 3264.
(18) Balazs, A. C.; Singh, C.; Lyatskaya, Y.; Chern, S. S.; Zhulina, E. B.; Pickett, G. T. *Prog. Surf. Sci.* **1997**, *55*, 181.
(19) Fleer, G.; Cohen-Stuart, M. A.; Scheutjens, J. M. H. M.; Cosgrove, T.; Vincent, B. *Polymers at Interfaces*; Chapman and Hall: London, 1993.
(20) Matsen, M. W.; Bates, F. S. *J. Chem. Phys.* **1997**, *106*, 2436.
(21) Pickett, G. T.; Balazs, A. C. *Macromolecules* **1997**, *30*, 3097.
(22) Tang, W. *Macromolecules* **2000**, *33*, 1370.
(23) McPherson, T.; Kidane, A.; Szleifer, I.; Park, K. *Langmuir* **1998**, *14*, 176.
(24) Drolet, F.; Fredrickson, G. H. *Phys. Rev. Lett.* **1999**, *83*, 4317.
(25) Schweizer, K. S.; Curro, J. G. *Adv. Chem. Phys.* **1997**, *98*, 1. (b) Schweizer, K. S.; Curro, J. G. *Adv. Polym. Sci.* **1994**, *116*, 319.

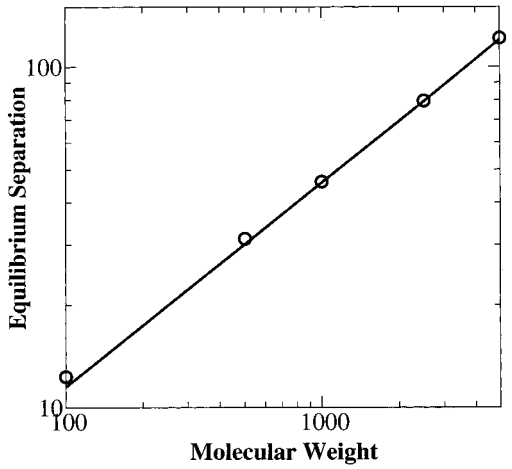

Figure 2. Athermal solvent, $\chi = 0$; uncharged chains, $\alpha = 0$. The equilibrium separation is determined by choosing L_Z so that the free energy in the system is minimized. For athermal chains, this should scale as the chain mean end−end separation or the Flory radius of swollen chains. The circles represent SCF calculations in the cylindrical lattice, and the solid line is a $N^{3/5}$ power law for comparison.

in Figure 1, has but a single polymer chain existing in a mean field generated by the solvent monomers (mol wt = 1) and itself. There are no other chains in the problem except the polyelectrolyte. Even still, the calculation has at least as much power as simple Flory-type arguments predicting the electrostatic necklace cascade of transitions.[11]

To show that our system is three-dimensional and properly models the behavior of a single chain, we have executed a preliminary calculation in which the bridging chain is electrostatically neutral and the solvent is athermal ($\chi = 0$). The results of this calculation are presented in Figure 2. For each molecular weight investigated ($N = 100-5000$), we determined the separation of the plates for which the free energy of the bridging chain is minimized. As in the original argument of Flory,[26] the fact that each end of the chain is anchored on opposite surfaces generates an entropic attractive interaction that causes the plates to swing together. Given that there are N monomers permanently trapped between the plates, as they come closer, the monomer density between the plates increases, thus giving rise to a repulsive interaction. These tendencies should balance for a plate separation that scales as $R_f \sim N^{3/5}$, the Flory radius in three dimensions. As seen in Figure 2, this three-dimensional, single-chain scaling holds over the entire range of the calculation. Thus, while the spirit of SCF calculations is violated by considering a single chain tethered between the plate surfaces, the agreement with scaling is a powerful validation of this "single-chain" SCF calculation.

The parameters of the system are given schematically in Figure 1. Our lattice has cylindrical geometry with azimuthal symmetry about the central axis. The lattice sites are labeled by $\vec{r} = (r, z)$, with $1 < r < L_R$, and $1 < z < L_Z$, and the basic unit of length is the monomer size, σ. Each lattice site accounts for a three-dimensional annular volume. A polymer of molecular weight N has its first monomer held at the lattice site $\vec{r} = (1, 1)$, and its Nth monomer held at $\vec{r} = (1, L_Z)$. No polymer segments are allowed to penetrate the circular surfaces at $z = 1$ or $z = L_Z$, and no monomers are allowed to penetrate the outer surface of the cylinder, $r = L_R$. We choose the polymer−wall interaction to be characterized by the same polymer−solvent χ parameter[27,28] so that the adsorption and desorption of chain segments will not affect the calculation. Thus, all surfaces are nonadsorbing. Additionally, each polymer segment is electrostatically charged with a fraction α of an electronic charge, e. Taking $e^2/\sigma/\epsilon \approx kT$ (where ϵ is the dc dielectric constant of the solvent), as is appropriate for water as the solvent,[29] we add an extra term to the polymer segment potential:

$$U_P = U_{hc} + \chi\langle\phi_S\rangle + \alpha^2 \int d\vec{r}\, d\vec{r}' \frac{\phi_P(\vec{r})\phi_P(\vec{r}')}{|\vec{r} - \vec{r}'|} \quad (3)$$

where the subscript P denotes a polymer quantity and the subscript S denotes a solvent quantity. Thus, we seek self-consistency for a bridging, charged chain in controllable solvent conditions.

It should be pointed out that in all cases, we merely fix the controllable parameters of the system (N, α, χ, L_R, and L_Z) and determine the location of the interior monomer segments in thermal equilibrium. We make no assumptions as to the number of "beads" on the conformation or to their location or size. Apart from the assumptions of the SCF model (a chain exists in a mean field determined by its own conformation, and the chain exists on a lattice with azimuthal symmetry about the center axis and incompressibility, eq 2), the calculation is without many of the a priori assumptions of the simple qualitative model used to originally justify the possibility of a cascade of necklace transitions.[11]

Qualitative Model: Cascade

This qualitative model is based on the following physically reasonable arguments.[11] The chain is assumed (Figure 1B) to be stretched out a length, L_Z, and to be composed of a number, n_b, of spherical beads of radius r_b, equally spaced and connected by stretched strings of length l. Furthermore, we assume that solvent conditions are so poor that the beads are composed entirely of polymer segments, and thus, the strings are fully stretched pieces of chain with a lateral size on the order of σ. Two important constraints can be placed on the polymer conformation:

$$N\sigma^3 = n_b r_b^3/\sigma^3 + (n_b - 1)l/\sigma \quad (4)$$

$$L_Z = n_b(r_b + l) - l \quad (5)$$

Here, we explicitly suppress all geometric factors of order unity (in contrast to the development in ref 11 and refs 13 and 14) to clarify the presentation and to emphasize that this model (and the original one proposed in ref 11) can only give qualitatively correct results. Essentially, we have that every monomer in the chain is either in a bead or in a string and that the lengthwise span of the chain, L_Z, is composed of the required number of beads and strings. The approximate free energy of the chain has two terms, one arising from the poor solvent and excluded volume interactions (equivalently, the surface interactions where polymer segments come into contact with solvent) and one arising from the electrostatic interactions. The surface interactions can be written as (again, suppressing

(26) deGennes, P.-G. *Scaling Concepts in Polymer Physics*; Cornell University Press: Ithaca, NY, 1979.

(27) Singh, C.; Zhulina, E. B.; Gersappe, D.; Pickett, G. T.; Balazs, A. C. *Macromolecules* **1996**, *29*, 7637.

(28) Chern, S. S.; Pickett, G. T.; Zhulina, E. B.; Balazs, A. C. *J. Chem. Phys.* **1998**, *108*, 5981.

(29) Grossberg, A. Y.; Khokhlov, A. R. *Statistical Physics of Macromolecules*; American Institue of Physics: New York, 1994.

numerical prefactors of order unity):

$$F_{\text{surf}} = n_b r_b^2 \gamma + \gamma l \sigma \tag{6}$$

Here, we take into account the surface area of each bead, weighted by the polymer−solvent surface tension, γ, and the free-energy cost of fully stretching the strings in the presence of a bad solvent. The electrostatic energy can be written as

$$F_{\text{es}} = n_b \frac{q_b^2}{r_b} + \sum_{i \neq j} \frac{q_b^2}{r_{ij}} \tag{7}$$

where q_b is the charge per bead; $q_b = r_b^3 \alpha$. The first term estimates the self-energy of each bead, and the second term accounts for the electrostatic interactions between separate beads. It is assumed that the strings contain far fewer monomers than the beads, so that the electrostatic interactions between strings may be neglected. The total chain free energy is

$$F_{\text{tot}} = F_{\text{surf}} + F_{\text{es}} \tag{8}$$

and the equilibrium size and number of beads in the conformation are chosen to minimize F_{tot} subject to the constraints of eqs 4 and 5.

In the original work on this topic, several further approximations are made in order to deduce some global properties of the bead-necklace conformation. Namely, the monomers in the stretchers are neglected in eq 4, and the size of the beads is neglected in eq 5. Also, the electrostatic interaction is approximated as

$$F_{\text{es}} = \frac{q_b^2}{r_b} + \frac{(n_b q_b)^2}{L_Z} \tag{9}$$

Thus, a simple scaling form for the interaction energy is assumed: it scales as the total charge on the chain squared, divided by the overall size of the stretched chain.

Minimizing F_{tot} with respect to both n_b and L_Z under the constraints of eqs 4 and 5 and under the approximation of eq 9 gives rise to two scaling laws:[11]

$$L_Z^{\text{eq}} \approx n_b q_b = N\alpha \tag{10}$$

$$\alpha_{n_b \rightarrow n_b+1} \approx \sqrt{\frac{n_b}{N}} \tag{11}$$

Thus, the overall equilibrium size of the chain scales such as the total charge on the chain and the fractional charge at which there is a transition from a chain with n_b beads to a chain with $n_b + 1$ beads scales similarly to the inverse square root of the chain molecular weight. We check both of these scaling laws in the following section with our SCF numerical technique. Thus, as α is increased at constant N, there are successive transitions from conformations with 1 to 2 to 3, etc. beads. We leave unresolved the issue of the condensation of neutralizing counterions when the chains are strongly charged and focus instead on the underlying beaded conformations.

SCF Model: Cascade

Exploring the beaded conformations in our SCF formalism is straightforward. In all of the calculations below, the solvent−polymer interaction is kept at $\chi = 2$; that is, the solvent conditions are very poor (where as above $\chi =$ 0 is an athermal interaction and $\chi = 0.5$ represents Θ conditions for the electrically neutral polymer). We choose N and α and then the dimensions of the cylindrical lattice. L_R is chosen to be large enough to not affect the calculation, typically 20 lattice units (so that the cylinder has a diameter of 40 lattice units). Then, a scan is made whereby the upper and the lower plates are placed at various L_Z. At each L_Z, a visual inspection of the conformation of the polymer is made. Usually, for any given L_Z, there are multiple conformations to consider. For example, as in Figure 3, at $L_Z = 33$, both a three- and a two-bead solution to the self-consistent equations exist. In the ensemble of the calculation (L_Z is held fixed, and the interior monomers are allowed to arrange themselves), assigning the equilibrium conformation is merely a matter of numerically calculating the free energy, F, of the conformation.[19] The conformation with the lowest F is the equilibrium conformation, in this case the two-bead chain. Thus, for each pair of (N, α), a determination of the lowest energy conformation can be made. Apparently, three-bead conformations are slightly metastable in Figure 3, but an increase in α to 0.17 brings the three-bead conformations to the absolute minimum of free energy, as in Figure 4. By following the energies of the two- and three-bead conformations, the transition point between the conformations can be determined. Thus, as shown, there are successive transitions from one to two to three beads on a single bridging chain as the charge on the chain is increased. In Figure 5, we show the location of the 1→2, the 2→3, and the 3→4 transitions for a convenient array of α and N values. The prediction, eq 11, for the location of the cascade transitions is at least qualitatively confirmed with approximately the correct power-law behavior.

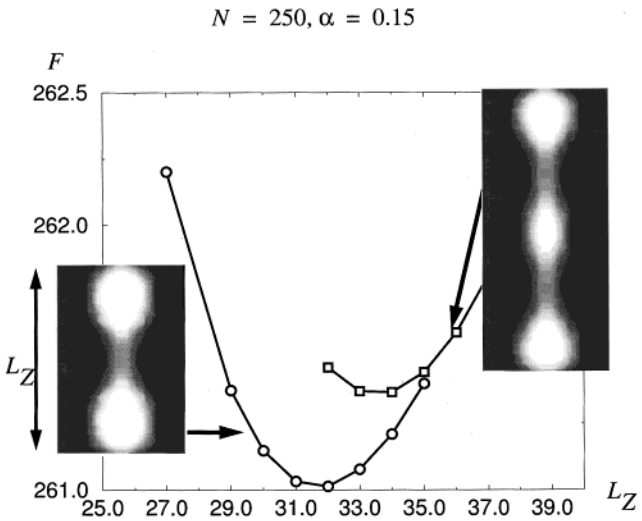

Figure 3. Bead conformations, SCF calculations. For $N = 250$ and $\alpha = 0.15$, successive scans over L_Z allow the determination of those plate separations at which the two- and three-bead conformations are in mechanical equilibrium. The two-bead conformation has a minimum of the chain free energy for $L_Z = 32$, while the three-bead conformation has its minimum at $L_Z = 33-34$. Clearly, the mechanically stable three-bead conformation costs more free energy than the mechanically stable two-bead conformation and hence is unstable. Thus, we identify the phase point (N, α) = (250, 0.15) with the two-bead phase. Chain conformations are shown, with black showing high solvent density and white showing high polymer density. The density in the center of the globules is ≈0.9 polymer.

The scaling prediction for the overall equilibrium size of the chain states that the main variation in L_Z^{eq} scales as the total charge = αN on the chain. Figure 6 shows the equilibrium size, over many chain conformations and

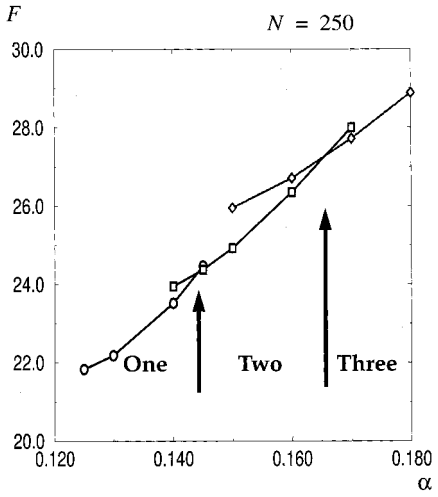

Figure 4. Transitions in α. Here, we show the free energy of the mechanically stable one-, two-, and three-bead conformations for $N = 250$ as a function of α. A linear function of α has been subtracted from these free energies to highlight the transitions but of course does not affect their locations. At each α, the bead conformation with the lowest free energy is the equilibrium structure to be expected for bulk, ungrafted polyelectrolytes. One-, two-, and three-bead domains are as marked.

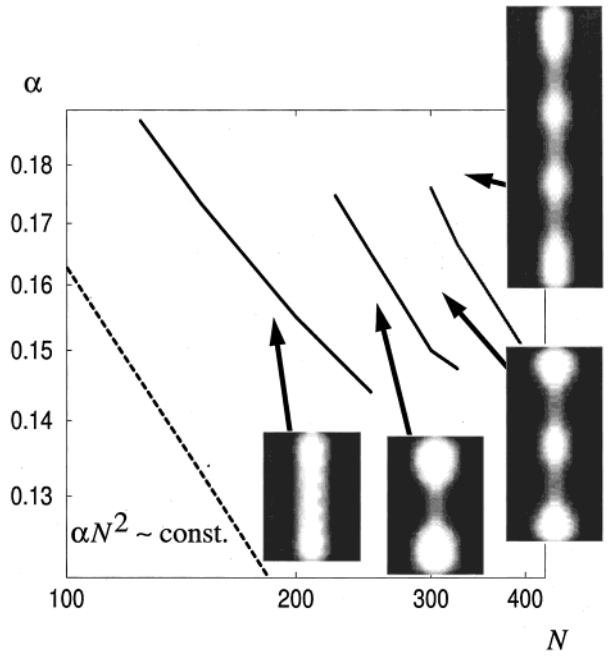

Figure 5. Diagram of states. Here, we demonstrate the necklace cascade of transitions. The lines represent first-order phase boundaries between the states with one, two, three, and four beads. The transitions occur with $\alpha N^{1/2} \approx$ constant, in accordance with eq 11. Inset in the figure are typical conformations from our SCF calculations that clearly demonstrate the validity of the "bead-and-string" hypothesis for the necklace transition. The SCF profiles show a cross-section of the cylindrical lattice. The corresponding three-dimensional structures can be generated by rotating these profiles through their long, central axis.

combinations of N and α, of the charged polymer, and there is a striking confirmation of the scaling prediction (eq 10). Note that the data in Figure 6 agrees only with the leading power-law dependence predicted in ref 11. It would seem that a more accurate fit to the data could be had by modeling the data as linear with a nonzero x-axis intercept. The fact that the data does not extrapolate

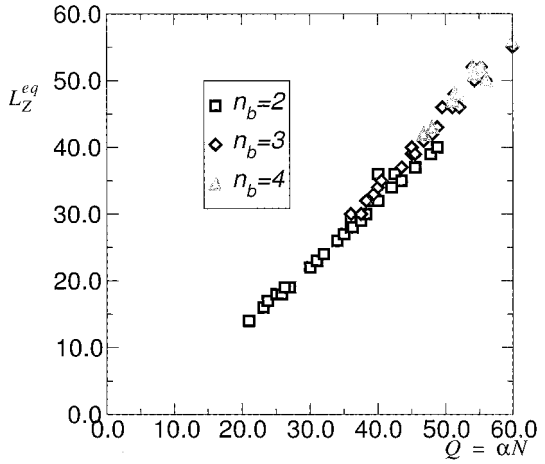

Figure 6. L_Z^{eq} vs $Q = \alpha N$. The scaling prediction, eq 10, is verified in our model. Plotted is the value of L_Z^{eq} for all multibead ($n_b = 2$, 3, or 4) conformations in the study vs $Q = \alpha N$, the total charge on the chain.

to zero (that is, zero charge leads to zero end−end separation) is a manifestation of the fact that the chain itself occupies a finite volume. For molecular weights in the range of 100−400 used in this study, the size of a completely collapsed globule is on the order of 6−7, clearly the correct order of magnitude to explain the curious disagreement with the scaling prediction. This illustrates the power of the numerical SCF method. The fact of the matter is that the scaling argument of ref 11 is not powerful enough to predict more than the leading power-law dependence of L_Z^{eq}. The SCF calculation captures this feature automatically. Thus, without making a priori assumptions about the nature of the conformations of the chain (apart from assuming that the chain ends in equilibrium are far apart so that our bridging conformations will mimic those of chains in the bulk), the chains manifestly self-organize into "folded" conformations under the influence of just two types of interactions and two types of monomers. We now turn to the crucial issue of the means of detecting these transitions experimentally.

Numerical AFM Experiment: Constant Tension

The presence of "electrostatic beads" in a dilute solution of poorly soluble, charged macromolecules can be detected through a thorough examination of isotropic scattering data spanning many length scales. However, with the advent of single-molecule control and imaging, it is possible to do far more than deduce length scales from scattering data. In the absence of direct visualization of native chain conformations, there are a host of mechanical tests that can be made of the theory, in part inspired by the nature of the SCF calculations[18] we offer here and first suggested in refs 13 and 14. The bridging geometry of our calculation is closely related to an AFM single-chain traction experiment. Here, one end of the chain is grafted on an immobile surface, and the other is grafted to the cantilever arm of the AFM. While it is most natural to fix the end−end separation of the chain in these calculations, it is most natural in an actual experiment to hold not the separation but the tension between the chain ends constant. Thus, to make contact between our calculations and an actual experimental signature for the traction-induced transitions requires taking our "constant L_Z" information and producing "constant chain tension" predictions. This requires nothing more complicated than the common tangent (equivalently "equal areas") construction of Maxwell.

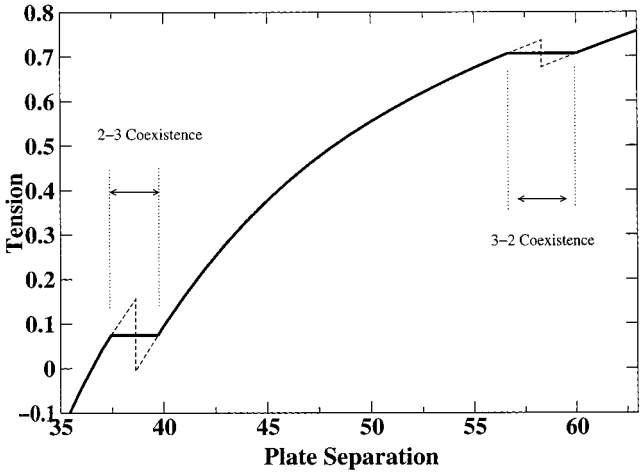

Figure 7. Traction-induced transitions, SCF. Results of SCF calculations on an $N = 300$, $\alpha = 0.15$ chain. The force required to hold the plates at a particular L_Z depends on the number of beads on the chain conformation. Thermodynamic stability requires that this force profile be monotonic as L_Z increases, but at each transition, the tension drops discontinuously. Maxwell constructions are required, and the transition from $n_b = 2$ to $n_b = 3$ at $L_Z = 38$ becomes a relatively wide coexistence zone. Similarly, at higher tensions, the middle bead on the conformation is destroyed in a first-order transition, again with a wide coexistence region. In an AFM experiment, there should be a sizable jump in the tip−surface separation during such a transition.

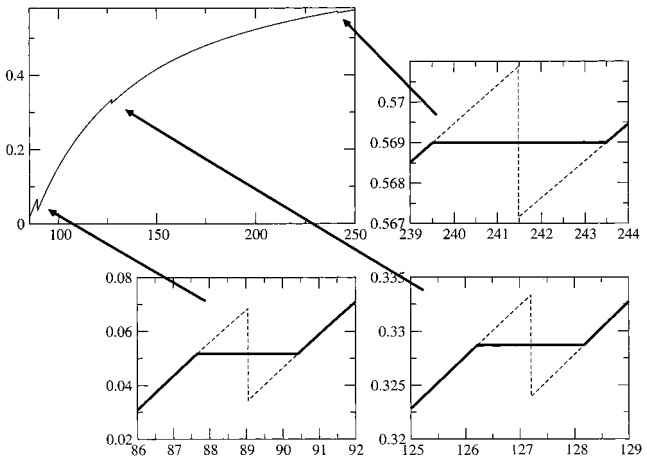

Figure 8. Traction-induced transitions, scaling model. Results from the qualitative scaling picture, showing coexistence-widened transitions from $n_b = 6$ to $n_b = 7$ to $n_b = 8$ and then back to $n_b = 7$. A spectrum of transitions should be visible in an AFM experiment. The model parameters for this calculation are $N = 500$, $\alpha = 0.1$.

Figure 7 shows the signatures that can be expected in either case (tension fixed or separation fixed). The tension, defined as $\partial F/\partial L_Z$, is shown as a function of plate separation for $N = 300$ and $\alpha = 0.15$. In the SCF fixed-L_Z calculations, at $L_Z = 38$, the three- and two-bead conformations have the same free energy. The tension in the chain is quite different, however, even though these conformations have the same free energy. The two-bead tension is considerably higher than the three-bead tension, so that increasing L_Z through the transition should give the dashed-line tension response. That is, there should be a sudden drop in the tension at the transition.

The same underlying two to three bead transition should exist in the constant tension ensemble of an AFM experiment. Here, however, the tension is held fixed, and mechanical stability requires that the tension be an increasing function of plate separation, L_Z. Thus, the response to be expected in the AFM is characterized by the heavy solid line in Figure 7. That is, as the applied tension is increased from slightly below 0.08 (in thermal units giving the basic scale of tension as $kT/\sigma \approx 10^{-11}$ N at room temperature), the separation of the AFM tip from the immobile surface should jump discontinuously from $L_Z = 37$ to 40. This discontinuity, on the order of 10% of the typical end−end size of the unperturbed chain, should be easily measurable. The "unphysical" region of $L_Z = 36-40$ is merely that region of separations for which both the two- and the three-bead conformations are metastable. If it could be arranged to maintain the tension at its transition value and also the average value of L_Z to be within this forbidden region, the lever rule will determine the ensemble average of the resulting conformation (i.e., how often the three-bead vs the two-bead conformation appears).

It should be noted that the curves shown in Figure 7 represent thermodynamic equilibrium only. The tension is locally an increasing function of extension everywhere except at the transition point where it is discontinuous (constant L_Z ensemble). Therefore, there is never a point at which the two-bead structure becomes linearly unstable to small-shape fluctuations leading to the transition to the three-bead state. The transition from two to three beads will thus always be characterized by an activation energy and hence a kinetic barrier. Thus, sizable hysteresis could be observable in real experiments, magnifying the signatures of these tensile bead transitions.

Given the model defined by eqs 4−8 (yet relaxing the extra assumptions in eq 9), it is also possible to track the traction-induced cascade of transitions between different beaded states. Here, the numerical prefactors that have been neglected in the model will surely affect the numerical results, but the qualitative features of the model are valid and agree with those set forth in refs 13 and 14. As in Figure 8, mechanical instabilities occur near the transitions between, in this case, the native $n_b = 6$ and the excited $n_b = 7$ states. Here, $N = 500$ and $\alpha = 0.1$. There are transitions from $n_b = 6$ to 7 and then to $n_b = 8$ and then back to $n_b = 7$. Each transition in this qualitative model has a jump in separation under constant tension conditions of ≈2% of the native conformation size and thus is easily detectable with current AFM techniques.

One final note concerns the curious "re-entrancy" of the tension-induced transitions. In the example presented here, adding tension to the chain induces a transition from a six-bead structure, to a seven-bead structure, to an eight-bead structure, and then back to the seven-bead structure. This re-entrancy is a general feature of the tension-induced configuration diagrams in refs 13 and 14.

It should be pointed out that these single-chain AFM techniques offer many advantages over analyzing the collective scattering from dilute solution. The measurement is unaffected by polydispersity. The location of the cascade transition points depends strongly on the molecular weight of the polyelectrolyte, so that many different bead-chain conformations are averaged over in a scattering experiment. Thus, the scattering signature of these transitions is extremely hard to detect. There is no such constraint with single-chain experiments. Not only is the molecular weight fixed for the chain under study, but it is extremely well-characterized by simply extending the chain to its full extent. Also, the cascade of transitions proposed in ref 11 results in a similar tension-induced set of transitions for the single chain under study in refs 13,

14, and 18. Coupled with a direct visualization of the charged chain, this technique will offer a direct, incontrovertible check on these theoretical discussions. The experimental details of neutralizing the AFM tip and suitably grafting the polyelectrolyte are complicated but offer yet another possible control on the transitions by applying a controllable voltage across the chain. This electromechanical method of detecting and inducing the shape changes of the "necklace-bead" transition will be the subject of further theoretical study.[30]

(30) Pickett, G. T. Manuscript in preparation.

Conclusion

We have studied the native conformation of bridging poorly soluble yet charged polyelectrolytes. The necklace-bead cascade of transitions as well as the mechanical means of inducing and detecting the transitions is evident. The calculation suggests a feasible experiment to settle the matter of the solution conformation of such chains.

Acknowledgment. G.T.P. gratefully acknowledges the support of the California State University and the Council for Undergraduate Research.

LA001034N